Reconfigurable Actuator-Sensor Arrays for the Active Control of Sound

Donald J. Leo
CSA Engineering
Palo Alto, California 94303-3843

Jonathan P. How
Department of Aeronautics and Astronautics
Stanford University
Stanford, CA 94305

Smart Structures and Materials:
Smart Structures and Integrated Systems
San Diego, CA
March 1997

Report Documentation Page

Form Approved
OMB No. 0704-0188

1. REPORT DATE	2. REPORT TYPE	3. DATES COVERED
MAR 1997		**00-00-1997 to 00-00-1997**

4. TITLE AND SUBTITLE	5a. CONTRACT NUMBER
Reconfigurable Actuator-Sensor Arrays for the Active Control of Sound	5b. GRANT NUMBER
	5c. PROGRAM ELEMENT NUMBER
6. AUTHOR(S)	5d. PROJECT NUMBER
	5e. TASK NUMBER
	5f. WORK UNIT NUMBER
7. PERFORMING ORGANIZATION NAME(S) AND ADDRESS(ES) **CSA Engineering Inc,Palo Alto,CA,94303-3843**	8. PERFORMING ORGANIZATION REPORT NUMBER
9. SPONSORING/MONITORING AGENCY NAME(S) AND ADDRESS(ES)	10. SPONSOR/MONITOR'S ACRONYM(S)
	11. SPONSOR/MONITOR'S REPORT NUMBER(S)

12. DISTRIBUTION/AVAILABILITY STATEMENT
Approved for public release; distribution unlimited

13. SUPPLEMENTARY NOTES
Smart Structures and Materials: Smart Structures and Integrated Systems, San Diego, CA March 1997

14. ABSTRACT
see report

15. SUBJECT TERMS

16. SECURITY CLASSIFICATION OF:			17. LIMITATION OF ABSTRACT	18. NUMBER OF PAGES	19a. NAME OF RESPONSIBLE PERSON
a. REPORT **unclassified**	b. ABSTRACT **unclassified**	c. THIS PAGE **unclassified**	**Same as Report (SAR)**	**13**	

Reconfigurable Actuator-Sensor Arrays for the Active Control of Sound

Donald J. Leo[a] and Jonathan P. How[b]

[a] Project Engineer
CSA Engineering, Inc.
Palo Alto, CA, 94303-3843 *

[b]Assistant Professor
Davis Faculty Scholar
Department of Aeronautics and Astronautics
Stanford University
Stanford, CA 94305

ABSTRACT

A reconfigurable actuator-sensor array is demonstrated for the active control of sound and vibration. The concept is motivated by applications in which shaped polyvinylidene fluoride films are used as error sensors for feedforward and feedback noise control. The advantage of the present concept, as compared to a fixed-shape sensor, is that the reconfigurable array can be adapted on line to account for uncertain structural dynamics, making it a more effective error sensor for applications in which the structural dynamics are not accurately known *a priori*. The array developed for this work consists of twenty-two polyvinylidene fluoride film sensors and four multilayer piezoceramic actuators connected to a set of reprogrammable electronics. The reprogrammable electronics consist of two 16 × 1 digitally-programmable gain boards and a digital signal processor with two analog inputs and outputs. The gains on the sensor array are set via the digital I/O of the digital signal processor. An off-line, frequency domain technique is used to design modal filters with the array of film sensors. Feedback and feedforward control algorithms are then implemented to demonstrate the use of the actuator-sensor array for noise and vibration suppression. The results indicate that the reconfigurable array technique has merit for noise and vibration control, although a fully adaptive, on-line algorithm has yet to be implemented.

Keywords: Active Structural-Acoustic Control, Sensor Arrays, Actuator Arrays

1. INTRODUCTION

Adaptive feedforward control techniques have been utilized in the majority of active structura-acoustic control applications. These techniques, such as Filtered-X Least Mean Squares, require the use of an error sensor in the feedforward control algorithm. The error sensor measures the difference between the response due to the disturbance input and the response due to the control input, and the weights of the adaptive filter are varied to minimize the mean square error signal.

One application of adaptive feedforward control has been the broadband reduction of sound power radiated by vibrating structures. Unlike local control of sound using microphones placed in the acoustic field, reducing the radiated sound power results in a global reduction of the sound pressure due to a vibrating structure. Unfortunately, though, the global reduction of radiated sound power is complicated by the lack of an appropriate error sensor for adaptive control algorithms. As discussed in Pierce, the sound power radiated by an acoustic source is equivalent to the spatial integral of the acoustic intensity over a surface that encloses the source.[1] Adhering to the strict definition of sound power, it would seem that a spatial array of error sensors is required to sense and control the sound power radiated by an acoustic source.

Recent results have shown that reducing structural sound power radiation is possible using error sensors located on the structure itself. It is well known that the sound power radiated from a structure is related to

* Current address: Mechanical, Industrial, and Manufacturing Engineering Department, Nitschke Hall, University of Toledo, Toledo, OH 43606-3390

SPIE Vol. 3041 • 0277-786X/97/$10.00

the radiation efficiencies of the structural modes.[2–4] This concept was the basis of the work by Clark and Fuller, in which polyvinylidene flouride strips were bonded to a plate and used as error sensors for adaptive least-mean square (LMS) control.[5] In Clark and Fuller's work, the strips were simply rectangular pieces of film bonded along the length in both directions on the plate. The length and placement of the film strips were such that the inefficient radiator modes were spatially filtered from the error sensor measurement.

A more sophisticated approach was developed specifically for the control of radiated sound power. In two recent papers, Snyder and Tanaka demonstrated that shaped polyvinylidene flouride films could be used for the broadband reduction of radiated sound power.[6,7] The PVDF films were shaped such that they measured a group of efficient radiator modes, where the shape of the film sensor was determined from the relative magnitudes of the modal contributions to the radiated sound power. The relative modal contributions were computed from an analysis that required knowledge of the structural mode shapes.

Both of these approaches represent fixed-shape solutions to the control of radiated sound power from plates. In the work by Clark and Fuller, simple shapes were used to filter out the response of modes that radiated sound inefficiently. The shaped sensor approach developed by Snyder and Tanaka, albeit more sophisticated, required *a priori* knowledge of the structural mode shapes and the acoustic environment before the shaped sensor can be designed. If the modes shapes are not known accurately, or if the mode shapes change during operation, then the predetermined shape of the film would not be an effective error sensor for sound power reduction.

The concept tested in this paper circumvents the problems inherent to a fixed-shape error sensor. In this work, an array of PVDF sensors was bonded to a flexible plate and connected to a reconfigurable set of electronics. The electronics included two 16 × 1 gain arrays constructed from digitally-programmable analog components. The gains can be reprogrammed through the digital input/output of the digital signal processor to vary the weightings on each of the sensor outputs.

The reconfigurable array concept is shown in Figure 1. Multiple sensors are bonded directly to the structure and connected to the gain array. The gain array condenses the large number of sensor signals into a smaller number of signals that are sent to the input of a digital signal processor. The DSP processes this smaller number of signals and generates commands to a gain array of actuators that apply forces to the structure. The DSP is also responsible for programming the gains of the actuator-sensor arrays so that the appropriate signal condensation or expansion is performed. This update is, however, performed at a much lower bandwidth than the feedback control.

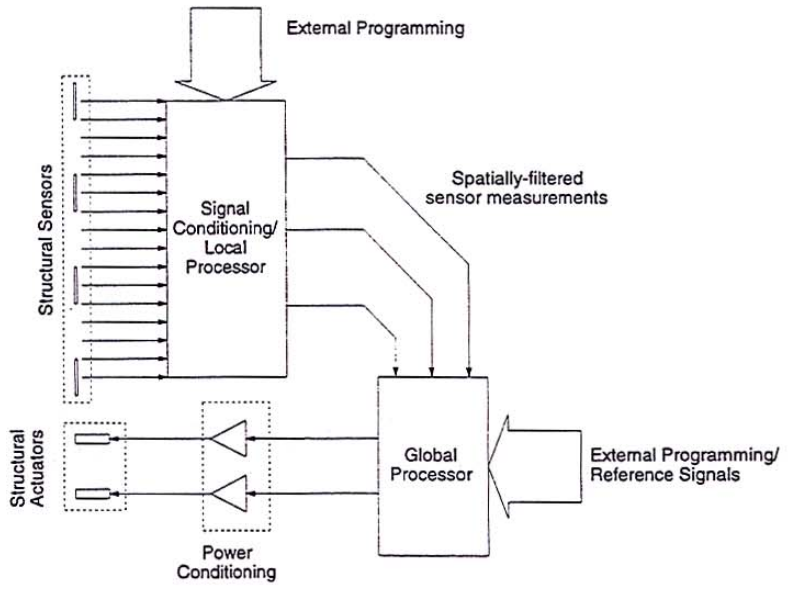

Figure 1. Reconfigurable array concept

There are two advantages of a reconfigurable array as compared to a fixed-shape error sensor. First, the reprogrammability enables the gains to be reconfigured in response to uncertain or changing dynamics. Unlike a fixed-shape sensor, the sensor array can be configured on-line in a situation where the efficient radiator modes are not known *a priori*. Secondly, the electronics are efficiently designed to maximize throughput and reduce phase lag due to discretization in the sample-and-hold process. Simple operations are performed by digitally-programmable analog electronics to eliminate phase lag associated with analog-to-digital or digital-to-analog conversion. More complex operations, such as implementation of feedback or feedforward control laws, is left to a DSP with a smaller number of inputs and outputs. Reducing the number of inputs and outputs enables higher sampling rates in the DSP, again reducing sample-and-hold phase lag.

The reconfigurable array developed in this work is an extension of the previous work by Clark and Fuller and Snyder and Tanaka. Sensors that filter out the response of inefficient modal radiators could be designed through proper weighting of the gain array. Likewise, sensors that output a signal related to the radiated sound power could also be designed using the analysis developed by Snyder and Tanaka. The benefit of the present approach is that reconfigurability enables the gains to be changed on line if the modes of the structure change or are uncertain.

The discussion in this paper concentrates on the hardware, filtering, and control aspects of a system connected to a single, relatively small, reconfigurable array. Thus one could consider this development to be focused on a particular spatial segment of a much larger structure. Future work will investigate the extension to include additional gains arrays for each spatial segment of the structure, and how to distribute these arrays over multiple regions of the structure.

This paper describes the results of a Phase I Small Business Innovation Research program sponsored by the Aviation Applied Technology Directorate. The objective of the program was to build a reconfigurable actuator-sensor array and test it in a series of noise and vibration control experiments. The next section of the paper discusses the sensors, actuators, and electronics used in the hardware demonstration. Following the discussion of the hardware, the experiments in spatial filtering the sensor measurements are described. A section on the feedback and feedforward control follows, and the final section summarizes the work and states the important conclusions.

2. RECONFIGURABLE ARRAY HARDWARE

The test article is a 0.914 m × 0.457 m × 1.58 mm (3' × 1.5' × 0.625") steel plate housed in a 10 cm (4") deep wooden cabinet. The plate is bolted to a steel frame at 2.5 cm spacings around all four edges. The frame is, in turn, screwed into the wood around the outside of cabinet to provide a solid edge condition for the plate. Figure 2 is a diagram of the hardware demonstration.

Twenty-two polyvinylidene flouride (PVDF) sensors are bonded onto the plate for sensing surface strain in the structure. Each film sensor is a rectangular strip 203 μm thick. Two sizes of PVDF sensors are used. In the long direction of the plate, twelve 7.1 cm × 1.55 cm are bonded along the centerline; in the short direction, ten 4.09 cm × 1.55 cm film sensors are bonded along the centerline.

The sensors were bonded to the plate with five-minute epoxy. Extra epoxy was placed on the outer edges of the film sensors to ensure the integrity of the bond. Poor bonding at the outer edges could cause the film sensors to peel of the surface easily, even well after the epoxy bond had set. Adding extra epoxy to the outer edges of the sensor eliminated this problem and produced a durable bond between the sensor and the outer surface of the plate. Due to the fact that ambient noise (such as flourescent lighting) can be a significant problem for a high impedance transducer such as PVDF film, the sensor signals were run through coaxial cable to minimize electromagnetic interference. The film sensors were bonded to the plate as shown in Figure 2. A numbering and lettering scheme was adopted. The long direction of the plate was denoted the X direction and the short direction of the plate was denoted the Y direction.

Four encapsulated multilayer piezoceramic actuators were also bonded to the surface of the plate using five-minute epoxy. Each multilayer actuator was 31.75 mm × 31.75 mm and 508 μ thick. Each of the four actuators was labeled as shown in Figure 2. During the bonding process, though, one of the piezoceramic actuators (PZT 4) cracked and was unusable for the duration of the experiments.

The control electronics are divided into two separate boards: a local processor that sums and weights the output of the sensor array, and a DSP-based global processor which implements the feedback and

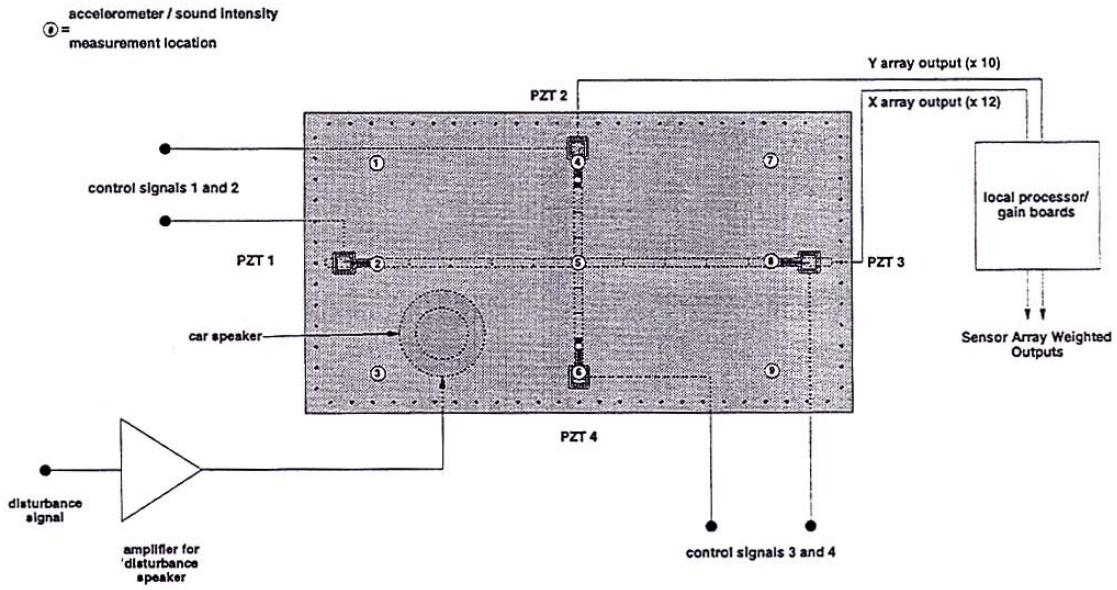

Figure 2. Diagram of the Phase I hardware demonstration.

feedforward control algorithm. The local processing electronics consist of two custom 16 input, 1 output digitally-programmable gain arrays. Each gain array board has three stages. The first stage is a bank of 16 charge amplifiers with a fixed gain of 303 μV/pC and a time constant of approximately 33 milliseconds. The time constant results in a highpass break frequency of approximately 5 Hz in the charge amplifier. The next stage was a bank of 16 bipolar unity gain amplifiers with 12-bit resolution. A lowpass filter with a break frequency of 800 Hz was placed in the digitally programmable gain stage to minimize noise feedthrough. All 16 channels of the current version of the array are located on one board, but future generations of the array could collocate each of the analog circuits with the sensor itself.

The gains of the amplifiers are set by the DSP through the digital I/O of the gain array board. The final stage is a unity-gain summation of the 16 individual signals with a lowpass filter of 1300 Hz. Each board is powered by a 15V bipolar supply and a 5V unipolar supply. The two gain boards were placed in a 36 cm $\times$ 25 cm aluminum chassis to ease the wiring burden and to increase the modularity of the sensor-actuator array. The chassis has BNC connectors for the inputs and outputs and banana plugs for the bipolar and unipolar power supplies. A picture of the completed chassis is shown in Figure 3.

The global processor is a DSP development system from Integrated Motions, Incorporated (IMI). The development system consists of a TMS320C31 DSP-based MX31 motherboard with 16-bit digital I/O and two daughterboards that contain analog-to-digital and digital-to-analog converters for two inputs and two outputs. The global processor is programmed via a 9-pin PC parallel port. Programming is done in C, compiled on the PC, and downloaded to the DSP through the parallel port. Code was written to program the gains of the array and to implement the feedback and feedforward control algorithms. Compilation and downloading of code took approximately 20 seconds when setting the gains and implementing a control algorithm.

Amplifiers for the multilayer PZT actuators were fabricated from previously designed printed circuit boards. The Burr-Brown OPA 544 power op-amp was used as a linear amplifier for the piezo drivers due to its ability to sink and source up to two amps of current and run from a bipolar 15 V power supply. For the current design, the gain of the amplifier is set at 10 and the bandwidth is approximately 1 kHz. A four-channel amplifier was built and placed into a chassis. The chassis contained BNC connections for the amplifier inputs and outputs as well as banana plug connections for the power supplies. A picture of the four-channel amplifier is shown in Figure 3.

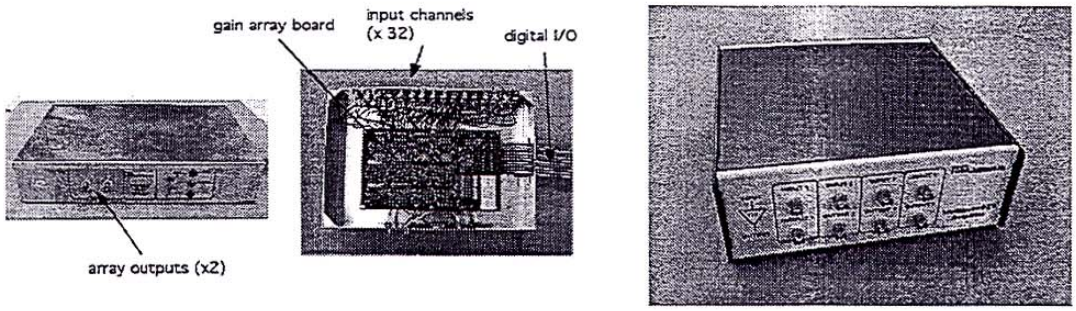

Figure 3. The sensor gain boards: front view (left) and top view (right).

3. SPATIAL FILTERING

Experiments were performed to demonstrate the spatial filtering capabilities of the reconfigurable array. The objective was to use the programmable electronics to shape the output of the arrays. The output was shaped to amplify or attenuate the response of particular structural modes for the purpose of feedback or feedforward control.

The first step was to obtain the input-output transfer functions between the three working piezoceramic actuators and the twenty-two PVDF sensors. The transfer functions were obtained over the range 0 to 600 Hz using a frequency resolution of 0.15 Hz. The 66 frequency responses were saved off line and stored in a array of the form:

The array of frequency responses were used for two types of spatial filtering. A "common sense" approach was used for simple problems in which the weights were chosen based on examining individual frequency response measurements. This approach amplified or attenuated the response of a set of structural modes. A more sophisticated least squares optimization was used to compute weights that minimized the error between a desired frequency response and the output of the array. This technique was used to design modal filters.

3.0.1. "Common Sense" Approach to Spatial Filtering

Limited knowledge about the structural dynamics was used to weight the array such that the response of certain structural modes is amplified or attenuated. An example of this is shown in Figure 4. The left plot in Figure 4 is a magnitude and phase plot for two of the PZT-to-PVDF frequency responses. Note how the resonance peaks at 42, 67, 98, and 132 Hz are approximately equal, yet the 42 Hz and 98 Hz peaks are out of phase with one another and the 67 Hz and 132 Hz peaks are in phase with one another. The relative phasing is related to the modal response at those frequencies.

The equivalence in the magnitudes and the difference in the relative phasing allows us to spatially filter these modes to amplify or attenuate the response at particular frequencies. For example, adding the two signals emphasizes the 42 Hz and 98 Hz peaks in the weighted frequency response. Similarly, subtracting the two sensor signals from one another emphasizes the 67 and 132 Hz resonant modes (see Figure 4).

A more sophisticated example of spatial filtering is shown in Figure 5. In this case, sensor gains on PVDFX2 through PVDFX6 are set equal to 1 and the sensor gains on PVDFX7 through X11 are set equal to -1. Also, the input is phased such that the same signal is sent to both PZT1 and PZT3. The resulting transfer function amplifies the response of the 42 Hz and 180 Hz structural modes and attenuates the other modes below 200 Hz.

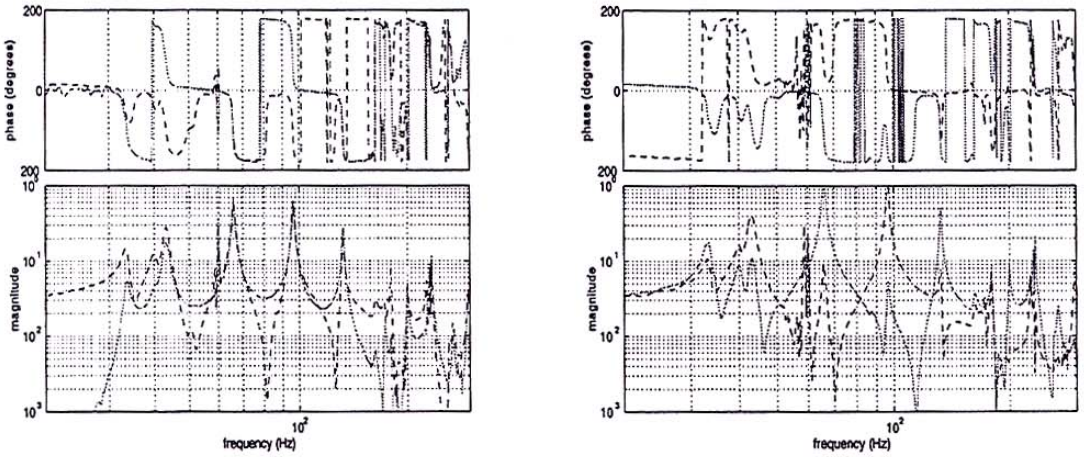

Figure 4. Magnitude and phase plots between the PZT inputs and two PVDF outputs (left) and the spatially filtered signals (right)

A similar result is obtained when filtering the sensors in the orthogonal direction. Figure 5 also includes a magnitude and phase plot between PZT2 and a weighted combination of sensors in the Y direction. Although the weighting scheme is similar to the previous case, the resonant modes that appear in the frequency response are different. For a weighted combination in the Y direction, three modes – 85, 95, and 120 Hz – are the dominant structural modes below 150 Hz.

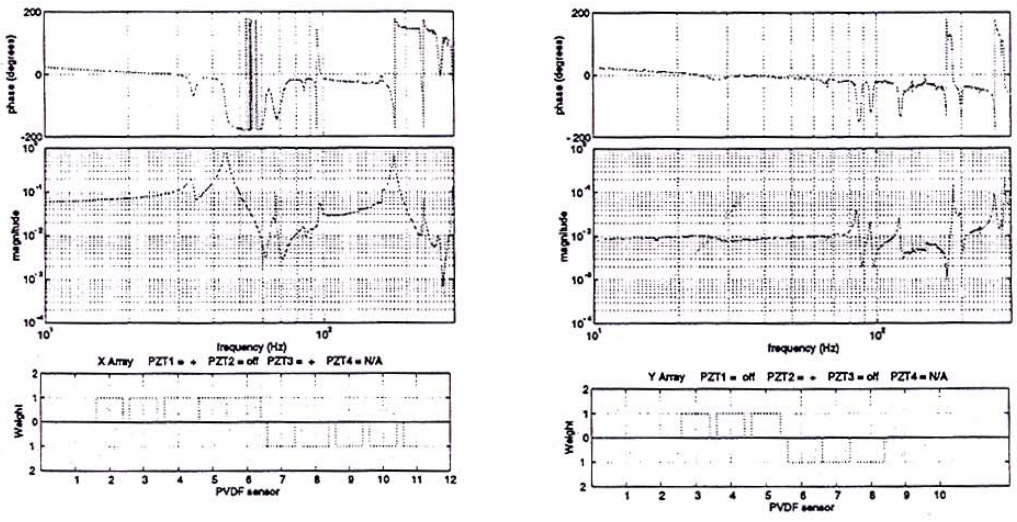

Figure 5. Spatial filtering for the 42 Hz and 180 Hz structural modes.

3.1. Modal Filtering

More sophisticated spatial filtering is possible using least squares optimization techniques to choose the sensor weighting coefficients. In particular, we can choose the coefficients such that the input-output frequency response emulates only a single-mode. This technique is called modal filtering, since the spatial weights of the sensors are chosen to isolate a single resonance mode in the frequency band.

The basis of the least squares optimization is the measured frequency response data between the PZT inputs and the PVDF outputs. For a specified set of inputs, we can write the output of the gain board as a weighted combination of frequency responses. For example,

$$X = x_1 F_{x1}(j\omega) + \ldots + x_{12} F_{x12}(j\omega), \tag{1}$$

would be the output of the X array, where x_i is the weighting coefficient of the i^{th} sensor and $F_{xi}(j\omega)$ is the frequency response between the i^{th} PVDF sensor and the inputs.

If we call the desired frequency response $F_d(j\omega)$, then we can write the problem as

$$x_1 F_{x1}(j\omega) + \ldots + x_{12} F_{x12}(j\omega) = F_d(j\omega), \tag{2}$$

In general, there are more data points in the frequency responses than there are sensor coefficients, therefore this problem becomes a standard least squares minimization of the form:

$$Ax = b, \tag{3}$$

where

$$A = \begin{bmatrix} \Re(F_{x1}(j\omega)) & \ldots & \Re(F_{x12}(j\omega) \\ \Im(F_{x1}(j\omega)) & \ldots & \Im(F_{x12}(j\omega) \end{bmatrix}, \qquad \in \mathcal{R}^{2N_{pts} \times 12} \tag{4}$$

$$x = [x_1 \ldots x_{12}]^T, \tag{5}$$

and

$$b = \begin{bmatrix} \Re(F_d(j\omega)) \\ \Im(F_d(j\omega)) \end{bmatrix}, \qquad \in \mathcal{R}^{2N_{pts} \times 12}. \tag{6}$$

The least squares solution to this problem is given by

$$x = (A^T A)^{-1} A^T b \tag{7}$$

of course, an equivalent problem can be posed for the Y array or for a combination of X array and Y array outputs. In general, the X array was used for the model filtering since the lower frequency modes were of interest for the feedback and feedforward control.

A simple least squares optimization code was written to compute the optimal weighting coefficients for a specified desired frequency response. The results of modal filtering for the 42 Hz mode are shown in Figure 6. The dashed line is the desired frequency response and the solid line is the measured output of the array with the optimal weights for the 42 Hz mode. The weighted output of the array emulates a single-mode system up until approximately 200 Hz, where the residues of the short wavelength modes enter into the frequency response. At frequencies greater than approximately 300 Hz, the spatial filtering has broken down and the response is dominated by the short wavelength modes.

A modal filter for the 233 Hz resonant mode is shown in Figure 6. Much the like the modal filter for the 42 Hz mode, the low-frequency response is dominated by the mode of interest. Below the mode of interest the sensor output has only negligible resonant dynamics.

There are two primary differences in the 42 Hz and 233 Hz modal filters. In contrast to the 42 Hz modal filter, the high frequency (short wavelength) modes are more prominent in the 233 Hz response relative to the mode of interest. For example, the resonance at approximately 340 Hz has a higher peak than the 233 Hz mode and it occurs only 1.5 times the frequency of interest. The weighting coefficients for the two modal filters are also quite different. For the 42 Hz modal filter, the spatial variation in the weights is much

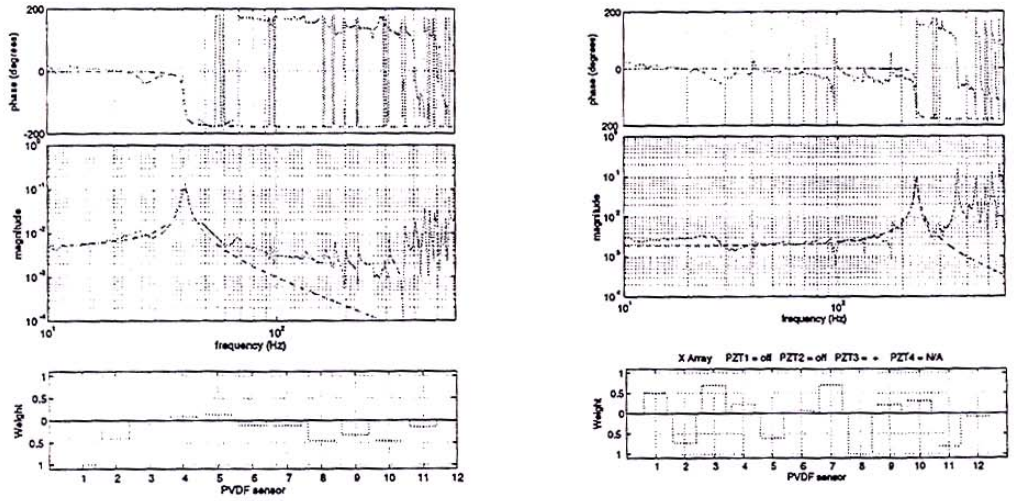

Figure 6. Modal filter for the 42 Hz resonant mode (left): desired transfer function (dashed) and measured weighted output of the sensor array (solid); Modal filter for the 233 Hz resonant mode (right)

smoother than in the case of the 233 Hz mode. This is to be expected because the wavelength of the 42 Hz mode is longer than the wavelength of the 233 Hz mode.

Modal filters were designed for six modes between 40 Hz and 250 Hz using the input to PZT3 and the output of the X array. The magnitude plots of the six modal filters are shown in Figure 7.

An equivalent least squares optimization process can be performed using the raw time date. This approach has the benefit that the data need not be converted into the frequency domain. However, there is the disadvantage that, since the sensors must be read sequentially with a repeated disturbance input, variations in the input noise excitation could corrupt the selection of the modal filter weights. The frequency domain technique typically averages out these noises more effectively, and thus, if feasible, would probably be the better approach.

As discussed earlier, the ultimate objective of the gain array is to provide a measure of the sound power radiated by the plate when excited by an acoustic source. This measure can be conveniently derived using the concept of power modes.[2–4] This approach results in a frequency dependent matrix $M(s)$ which captures the relative radiation efficiency of linear combinations of the structural modes. The relative efficiency is determined by the eigenvalues of $M(s)$ at a given frequency. The eigenvectors of the power mode matrix provide the appropriate linear combinations to use for the structural modes. These matrices $M(s)$ can be computed numerically for plates with simple boundary conditions.

As shown previously, we can develop estimates of the modal response of the system as $\hat{\phi}_k$, where

$$\hat{\phi}_k = \left[\alpha_{k1}, \ldots, \alpha_{km} \right] \begin{bmatrix} y_1 \\ \vdots \\ y_m \end{bmatrix} = \underline{\alpha}_k^T \underline{y} \tag{8}$$

y_i is the response of the ith PVDF sensor in the array, and $\underline{\alpha}_k$ are the array gains. We can then develop real-time estimates of the jth power mode for the system from our estimates of the modal response using

$$\hat{P}_j = \sum_{k=1}^{N} \beta_{jk} \hat{\phi}_k = \left(\sum_{k=1}^{N} \beta_{jk} \underline{\alpha}_k^T \right) \underline{y} \tag{9}$$

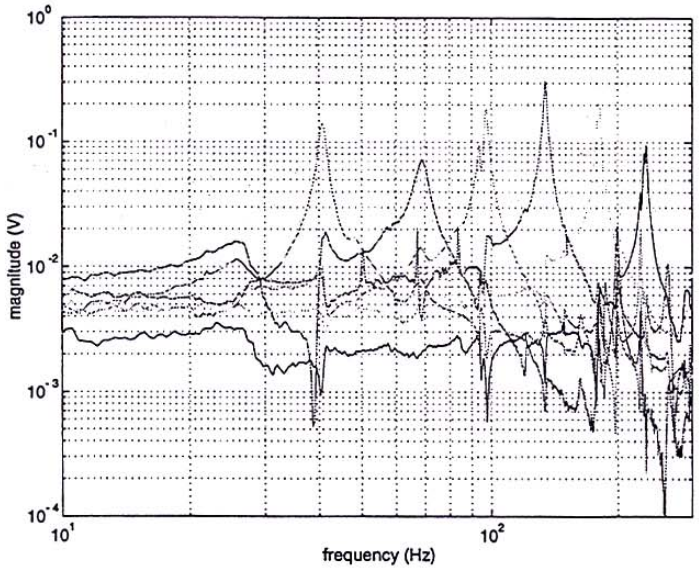

Figure 7. Measured magnitude responses of the six modal filters designed using the X array.

where the β_{jk} are determined from the eigenvector analysis of $M(s)$ at a given disturbance frequency, and N is the number of assumed structural modes. This expression gives the appropriate linear combination of the available sensor measurements to extract an estimate of the jth power mode for the system. Current work is focused on developing techniques for *in-situ* selection of the power mode coefficients β_{jk} for more complex systems.

4. Control Experiments

4.1. Broadband Damping using Feedback

The ultimate objective is to develop controllers that attenuate the sound radiated from the plate. However, as shown previously, the radiated sound can be related to the power modes of the system, and these power modes can, at a given frequency, be written as a linear combination of the structural modes. Thus the control objective really is to design compensators that efficiently attenuate the structural vibrations associated with these power modes. With this in mind, one of the objectives of the preliminary control work was to demonstrate that the sensor array could be used to isolate specific structural modes so that they can be attenuated. If this can be achieved, then it should also be possible to design controllers to attenuate linear combinations of these modes.

The controllers were designed using the piezoelectric actuators at both ends of the X-axis sensor array. The feedback was from the third and tenth PVDF sensors, which are symmetric with respect to the plate center. Models were developed for the control design by a system identification of measured data. The identification was performed using an Integrated Frequency-domain Observability Range Space Extraction and Least Square parameter estimation technique (IFORSELS).[8] The result was a 36th order model that matches the measured data very well up to 500 Hz. Note, however, that while this model is a very accurate representation of the measured data, changes in the operating conditions typically resulted in small errors when the model was compared to the dynamics of the actual system.

Controllers were designed for this two-input two-output system using robust $\mathcal{H}_2$ (LQG) techniques. Robustness was added to the controller to reduce sensitivity to errors in the modal frequencies of the first 5 modes. Robustness was included using de-sensitizing methods such as Sensitivity Weighted LQG and optimization methods such as Multiple Model.[9] The MIMO controllers designed using these techniques were reduced to 15th order and implemented at 3500 Hz on the IMI DSP.

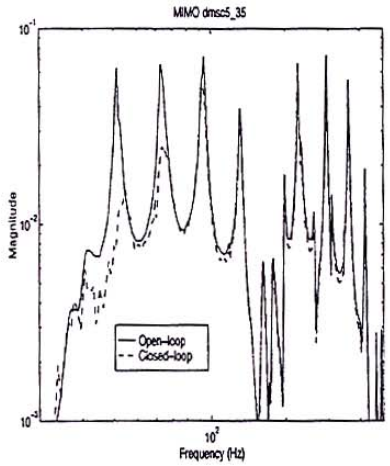

(a) Performance penalty on first two modes.

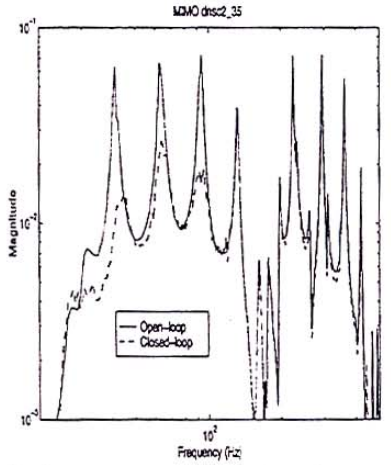

(b) Performance penalty on first three modes.

Figure 8. Feedback control results using gain array to modally filter the performance objective.

The objective function in the LQG design used the optimized array gains to isolate and penalize specific modes of the system dynamics. While this process of modal control is well known, the primary goal here was to demonstrate that we could use the array weights to select particular modes of a modally dense system. The cost function was augmented with a double pole roll-off (bandwidth 50 Hz, 0.707 damping) on the state cost to de-emphasize the high frequency response which is not filtered very well by the array.

The results for two typical MIMO controllers are shown in Figs. 8(a) and 8(b). The controller in Fig. 8(a) was designed to target just the first 2 modes of the system, while the one in Fig. 8(b) also included a penalty on the response of the third mode. Each controller was designed with the same control penalty within the LQG formulation. As expected, the controllers significantly increase the damping of the penalized modes. These results clearly show that the modal filtering of the array can be used to select particular modes of the system since, in the first case, there is very little attenuation of the third mode, and in both cases, there is no attenuation after the third mode. The next step is to design controllers that attenuate linear combinations of these modes and demonstrate the reduction in the sound power radiated. The entire array could also be used as the feedback sensor to further simplify the control design.

4.2. Narrowband Vibration Suppression using Feedforward Control

The Filtered-X LMS (FXLMS) algorithm was implemented for narrowband control using the six modal filters designed with the X array. Models of the secondary path (which improves the convergence of the FXLMS algorithm) were obtained from the measured data and a curvefit of the measured response was used as the plant model. The curvefits were performed using an optimization procedure that constrained the real part of the poles of the plant model to be in the right-half plane. This guaranteed the stability of the plant model. The specific reference used for the FXLMS algorithm was Kuo and Morgan.[10]

The external excitation source for the feedforward control problems was the external speaker housed in the cabinet. The speaker was driven at a narrowband tone and the vibration on the plate was measured at nine locations with accelerometers (see Figure 1). The array was configured such with the modal filter weights computed from the least squares minimization procedure described in the previous section. The FXLMS algorithm was turned on and the weights were allowed to converge before measuring the controlled response at the nine accelerometer locations. The six FXLMS control laws were implemented in the global processor at a sampling rate of 3500 Hz. A script file was written to output the C code for the FXLMS algorithm. This streamlined the procedure and made implementation of the algorithm more efficient.

The narrowband control results are shown in Table 1. The results represent the spatial average of the acceleration measurements at the nine locations on the plate. As Table 1 indicates, the FXLMS algorithm is most effective using the first and fourth modal filters. Almost a factor of 10 reduction is achieved in the

Table 1. Results of the Feedforward Control Experiments

Modal Filter	Analysis Frequency (Hz)	Open-loop RMS Acceleration (mg)	Closed-loop RMS Acceleration (mg)	RMS Reduction (dB)
1	41.02	110.5	12.7	18.82
2	66.01	173.3	74.7	7.30
3	94.53	399.7	472.2	-1.45
4	132.81	357.5	98.3	11.22
5	178.12	585.5	407.9	3.14
6	232.03	504.6	426.5	1.46

vibration levels on the plate for the 42 Hz modal filter. The performance is poor at the shorter wavelength modes of 178 and 233 Hz. The poor performance is attributed to the increasing wavelength and decreasing spatial resolution of the array at these frequencies.

4.3. Narrowband Sound Power Suppression using Feedforward Control

Narrowband sound intensity measurements were also made while using the FXLMS algorithm to control the 42 Hz structural mode. Using the disturbance speaker, the plate was driven at 41.02 Hz and nine sound intensity measurements were made at a point 5 cm above the plate.

Narrowband measurements were made due to the low confidence in the broadband intensity measurements. Measurements were made in the lab with no anechoic environment around the plate, therefore the reverberation (especially at such low frequencies) produced high levels of background noise in the intensity measurements. For narrowband inputs, though, a clear distinction between controlled and uncontrolled measurements could be made.

The reduction in magnitude of the sound intensity is shown more clearly in Figure 9. The reduction in sound intensity is greater than 15 dB at five of the nine locations and almost 30 dB at location 1. The sound intensity does increase by approximately 3 dB at location 4.

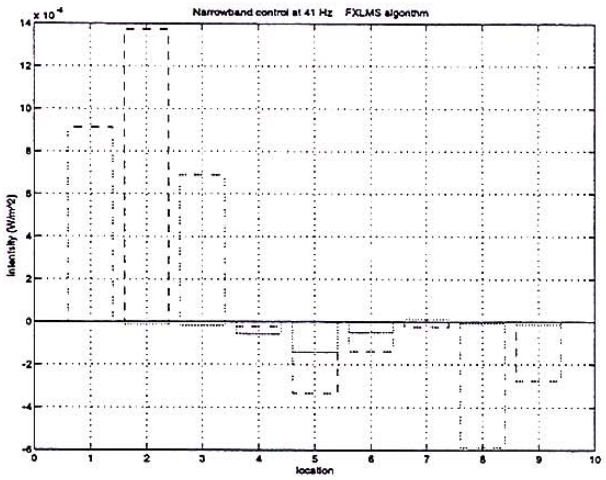

Figure 9. Magnitude of the sound intensity at nine locations above the surface of the plate.

5. SUMMARY AND CONCLUSIONS

The noise and vibration control experiments performed in this work demonstrated the merit of a reconfigurable sensor-actuator array. The reconfigurability of the array enabled the design of several types of spatial

filters, including the design of modal filters for the first six modes of a flexible plate. An advantage of the present concept was the decomposition of the control electronics into two stages: a digitally-programmable gain stage that performed simple weighting and summation of the sensor signals, and a digital signal processor which implemented the feedforward and feedback control algorithms. Decomposing the control electronics into two stages eliminated the need for a digital signal processor with a large number of inputs and outputs, thus increasing the throughput rate of the processor and decreasing phase lags due to sample-and-hold operations.

The next step in this work is to combine the array concept with a more detailed examination of active control of radiated sound power. The modal filtering methods will be extended to a more sophisticated on-line technique that automatically adapts the array weights such that the error sensor is correlated with the acoustic power output of the structure. The challenge for this work will be the design of an autonomous system that adapts itself in the presence of uncertain or time-varying structural dynamics.

ACKNOWLEDGEMENTS

This work was funded by the Small Business Innovation Research contract number DAAJ02-96-C-0013, sponsored by the Department of the Army. The technical monitor for the work was Mr. Don Merkley of the Aviation Applied Technology Directorate of Fort Eustis, VA.

REFERENCES

1. A. D. Pierce, *Acoustics*, Acoustical Society of America, New York, 1981 (reprinted 1989, 1994).
2. C. Wallace, "Radiation resistance of a rectangular panel," *Journal of the Acoustical Society of America* **51**, pp. 946–952, 1972.
3. M. Gomperts, "Sound radiation from baffled, thin, rectangular plates," *Acustica* **37**, pp. 93–102, 1977.
4. S. D. Snyder and N. Tanaka, "Calculating total acoustic power output using modal radiation efficiencies," *Journal of the Acoustical Society of America* **97**, pp. 1702–1709, 1995.
5. R. L. Clark, "Modal sensing of efficient acoustic radiators with polyvinylidene fluoride distributed sensors in active structural acoustic control approaches," *Journal of the Acoustical Society of America* **91**, pp. 3321–3329, 1992.
6. S. D. Snyder, N. Tanaka, and Y. Kikushima, "The use of optimally shaped piezo-electric film sensors in the active control of free field structural radiation, part 1: Feedforward control," *Journal of Vibration and Acoustics* **117**, pp. 311–322, 1995.
7. S. D. Snyder, N. Tanaka, and Y. Kikushima, "The use of optimally shaped piezo-electric film sensors in the active control of free field structural radiation, part 2: Feedback control," *Journal of Vibration and Acoustics* **118**, pp. 112–121, 1996.
8. K. Liu and D. W. Miller, "System identification by the ORSE technique with a finite number of data samples," in *Proceedings of the American Control Conference*, pp. 2310–2315, Inst. of Electrical and Electronics Engineers, Piscataway, NJ, June 1993.
9. S. C. O. Grocott, J. P. How, D. W. Miller, D. G. MacMartin, and K. Liu, "Robust control design and implementation on the Middeck Active Control Experiment (MACE)," *AIAA Journal of Guidance, Control, and Dynamics* **17**, pp. 1163–1170, Nov.–Dec. 1994.
10. S. Kuo and D. Morgan, *Active Noise Control Systems, Algorithms and DSP Implementations*, John Wiley and Sons, New York, 1996.